Materials Science and Engineering C 80 (2017) 135–140

Contents lists available at ScienceDirect

Materials Science and Engineering C

journal homepage: www.elsevier.com/locate/msec

Investigation on direct electrochemical and electrocatalytic behavior of hemoglobin on palladium-graphene modified electrode

Wei Chen [a,b,1], Xueliang Niu [a,1], Xiaoyan Li [a], Xiaobao Li [a], Guangjiu Li [b], Bolin He [a], Qiutong Li [a], Wei Sun [a,c,*]

[a] Key Laboratory of Tropical Medicinal Plant Chemistry of Ministry of Education, College of Chemistry and Chemical Engineering, Hainan Normal University, Haikou 571158, China
[b] College of Chemistry and Molecular Engineering, Qingdao University of Science and Technology, Qingdao 266042, China
[c] Key Laboratory of Soft Chemistry and Functional Materials of Ministry Education, College of Chemical Engineering, Nanjing University of Science and Technology, Nanjing 210094, China

ARTICLE INFO

Article history:
Received 4 March 2017
Received in revised form 17 May 2017
Accepted 20 May 2017
Available online 21 May 2017

Keywords:
Hemoglobin
Graphene-palladium nanocomposite
Direct electrochemistry
Electrocatalysis

ABSTRACT

Palladium-graphene (Pd-GR) nanocomposite was acted as modifier for construction of the modified electrode with direct electrochemistry of hemoglobin (Hb) realized. By using Nafion as the immobilization film, Hb was fixed tightly on Pd-GR nanocomposite modified carbon ionic liquid electrode. Electrochemical behaviors of Hb modified electrode were checked by cyclic voltammetry and a pair of redox peaks originated from direct electron transfer of Hb was appeared. The Hb modified electrode had excellent electrocatalytic activity to the reduction of trichloroacetic acid and sodium nitrite in the concentration range from 0.6 to 13.0 mmol·L^{-1} and from 0.04 to 0.5 mmol·L^{-1}. Therefore Pd-GR nanocomposite was proven to be a good candidate for the fabrication of third-generation electrochemical biosensor.

1. Introduction

Electrochemistry of redox proteins/enzymes is difficult to achieve due to the deeply buried of electroactive centers inside of their polypeptide structures [1]. To solve this problem multifarious chemically modified interfaces have been designed to improve the process of electron transfer [2]. Due to the similarities between the electron transfer on the electrode and on the biological membrane in living bodies, the investigation can be applied to understand the mechanism inside the biological system. Also the results can be used to build biosensors and bioreactors [3]. As a redox protein consisted of two α and two β polypeptides, hemoglobin (Hb) has the responsibilities to restore and transfer oxygen [4]. The shape of Hb is almost sphere with its molecular weight about 64,500 Da with the size of 6.5 × 5.5 × 5.0 nm. Because of its well-known structure, Hb is often selected as the model molecule in direct electrochemistry of protein and electrochemical sensors [5].

Ionic liquid (IL) is organic compound with specific electrochemical performances, which is widely used in electrochemistry with good stability, high conductivity, easy to dissolve and wide electrochemical window [6]. Carbon ionic liquid electrode (CILE) is defined as carbon paste electrode (CPE) that used IL as the binder and the modifier [7]. CILE exhibits the superior characteristics than CPE, including high conductivity, certain catalytic activity and good anti-fouling ability. Therefore CILE is reported as the working electrode in electroanalysis [8–10].

With the development of nanoscience various nanomaterials and hybrid materials have been synthesized and used in different fields including catalyst, sensors, drug and gene delivery, photodynamic therapy, optogenetics, and so on [11–20]. Dhand et al. reviewed the methods and strategies for the synthesis of diverse nanoparticles and their applications [21]. Loh et al. summarized the delivery of gene materials with inorganic materials [22]. Therefore nanomaterials play important roles with various applications. Graphene (GR) is a carbon nanosheet that consists of single layer of carbon atom, which has many specific characteristics including high conductivity, low resistance, easy to produce and large surface area [23,24]. Due to its large surface area, GR can be decorated by other nanometerials to obtain nanocomposite that shows synergistic effects [25]. Nanosized Pd is a commonly used catalyst in the electrochemical reaction, which can lower the active energy and fast the electrochemical reaction due to its high activity. Maleki et al. applied nanosized Pd modified electrode for electrocatalytic determination of hydrazine [26]. Wang et al. fabricated a glucose sensor with porous Pd nanotubes on glassy carbon electrode (GCE) [27]. Yang et al. described the formation of Pd-based nanoporous metal with improved catalytic activity towards glucose oxidation [28]. Ke et al. prepared a Pd-decorated nanoporous gold/Ni foam electrode for the evaluation of H_2O_2 electroreduction [29]. Huang et al. proposed a ratiometric electrochemiluminescence (ECL) immunosensing method by introducing the lumiol/palladium nanoclusters@graphene oxide probe to the ECL immunosensor [30]. By decorating GR with nanosized Pd, Pd-GR nanocomposite exhibits

* Corresponding author at: Key Laboratory of Tropical Medicinal Plant Chemistry of Ministry of Education, College of Chemistry and Chemical Engineering, Hainan Normal University, Haikou 571158, China.
E-mail address: sunwei@qust.edu.cn (W. Sun).
[1] Wei Chen and Xueliang Niu are co-first authors.

http://dx.doi.org/10.1016/j.msec.2017.05.129
0928-4931/

the enhanced performance with the obvious synergistic effects. Shi et al. fabricated a Pd-GR catalyst modified GCE for 4-chlorophenol analysis [31]. Dong et al. prepared flower-like palladium nanoclusters on electrodeposited GR electrode for hydrogen gas analysis [32]. Kumar et al. used a Pd-GR nanocomposite modified GCE for electrochemical determination of ethanol [33]. GR related hybrid materials have also been used for the realization of direct electrochemistry of redox proteins. For example, Zhan et al. applied Co_2Al layered double hydroxide and GR nanocomposite on CILE surface for the immobilization of Hb [34]. Wen et al. constructed an electrochemically reduced graphene oxide and Hb modified GCE for the detection of nitromethane [35]. Mohammadrezei et al. used Hb-GR quantum dots-chitosan for

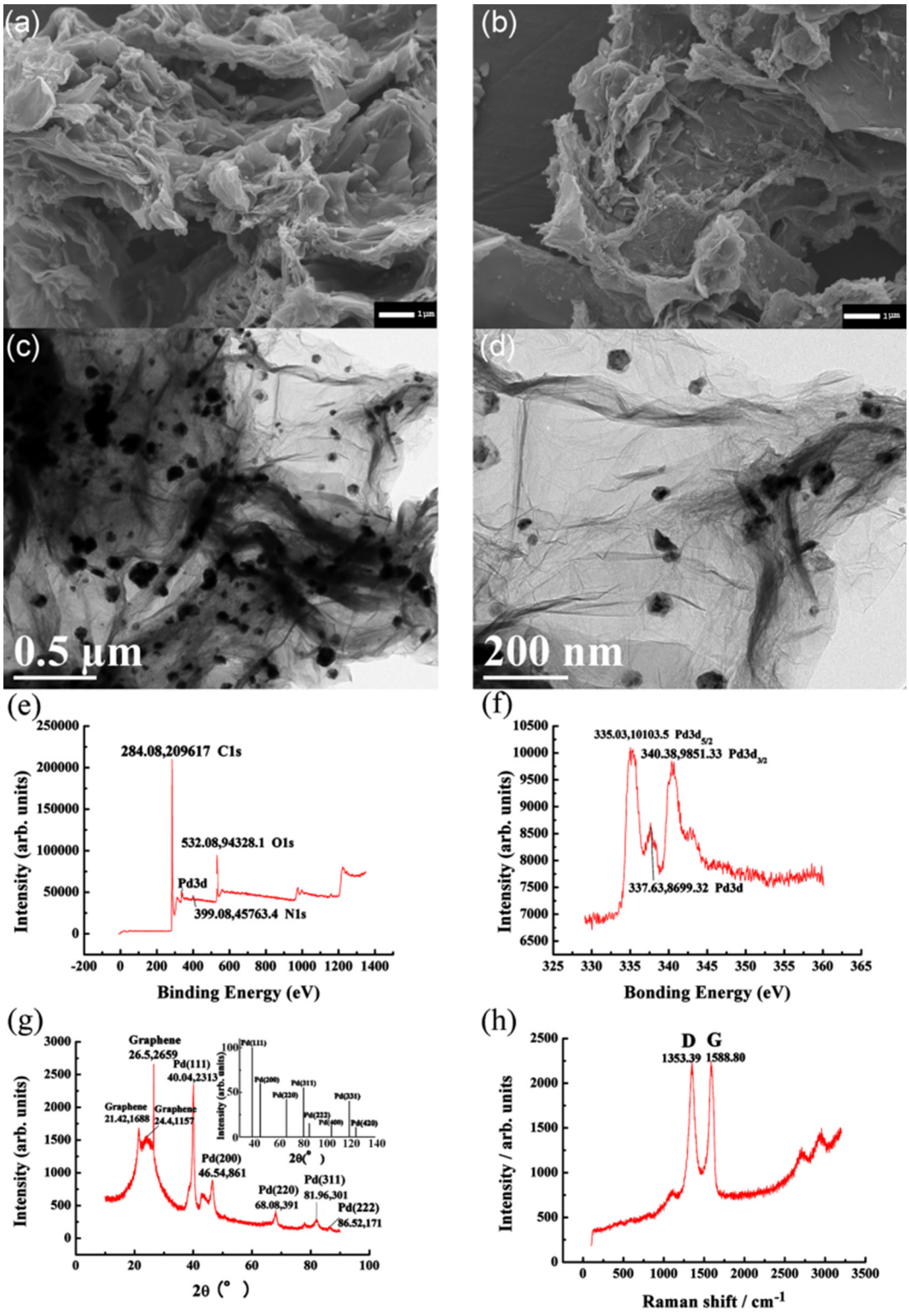

Fig. 1. SEM images of Pd-GR nanocomposite on CILE (a and b), TEM images of Pd-GR nanocomposite under different magnifications (c and d); XPS spectrum of Pd-GR composite (e); XPS spectrum of Pd in local zoom area (f); XRD pattern of Pd-GR nanocomposite (g), (inset was the standard XRP pattern of Pd); Raman spectrum of Pd-GR nanocomposite (h).

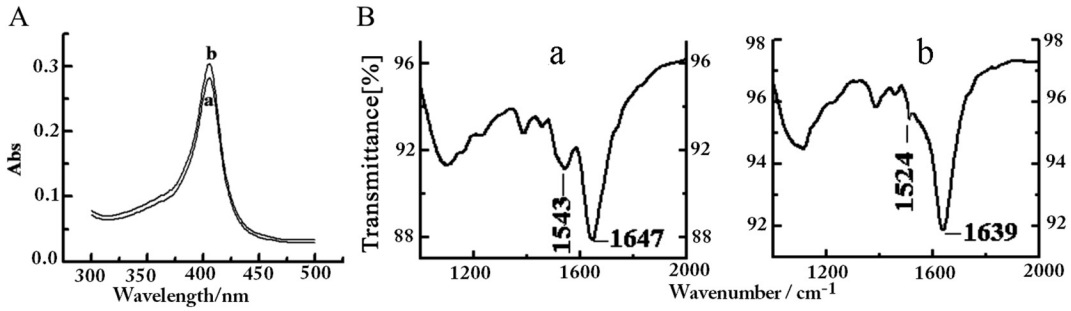

Fig. 2. (A) UV–Vis absorption spectra of (a) Hb solution and (b) Hb-Pd-GR mixture. (B) FT-IR spectra of (a) Hb and (b) Hb-Pd-GR.

biosensing detection of H_2O_2 in urine samples [36]. Zhao et al. investigated the electrochemistry of Hb with an IL-GR-NiO nanocomposite modified electrode [37].

In this paper Pd-GR nanocomposite was used to modify on CILE with the further immobilization of Hb by using Nafion as film material. Electrochemical behaviors of Hb on the electrode were investigated in detail with electrocatalysis to the reduction of different substrates performed. Also the proposed method was applied to the samples detection with satisfactory results.

2. Experimental

2.1. Instruments and reagents

A CHI 660D electrochemical analyzer (Shanghai CH Instrument, China) was used for electrochemical investigations. Voltammetric cell was composed of a three-electrode model with modified CILE (the working electrode), saturated calomel electrode (SCE, the reference electrode) and a platinum wire electrode (the counter electrode). UV–Vis absorption spectra was performed on TU-1901 double beam UV–Visible spectrophotometer (Beijing General Instrument Ltd. Co., China) with FT-IR spectra on Nicolet 6700 FT-IR spectrometer (Thermo Fisher Scientific Inc.,USA). Scanning electron microscopic (SEM) images were obtained on JSM-7600F instrument (JEOL, Japan) with transmission electron microscopy (TEM) on a JEM2010F transmission electron microscope (JEOL, Japan). X-ray diffraction (XRD) experiments were done on a D/Max-2500V X-ray diffractometer (Rigaku, Japan) with Cu-Kα radiation (λ = 1.54178 Å). A Raman spectrum was obtained on a LabRAM HR system using 532 nm lasers (Horiba, France) and X-ray photoelectron spectroscopy (XPS) was on an AXIS HIS 165 spectrometer (Kratos Analytical, UK).

Ionic liquid 1-hexylpyridinium hexafluorophosphate ($HPPF_6$, Lanzhou Yulu Fine Chem. Co., China), bovine hemoglobin (Hb, MW 64500, Tianjin Chuanye Biochemical Co. Ltd., China), graphite powder (average particle size 30 μm, Shanghai Colloid Chem. Ltd. Co., China), Nafion (5.0% ethanol solution, Sigma), Pd-GR nanocomposite (Nanjing XFNANO Materials Tech. Ltd. Co., China), trichloroacetic acid (TCA, Tianjin Kemiou Chemical Ltd. Co., China), sodium nitrite ($NaNO_2$, Yantai Sahe Chem. Ltd. Co., China) and medical facial peel (35%, Shanghai EKEAR Bio. Tech. Ltd. Co., China) were used as received. The supporting electrolyte was 0.1 $mol \cdot L^{-1}$ phosphate buffer solution (PBS), which was deoxygenized before experiment.

2.2. Preparation of Nafion/Hb-Pd-GR/CILE

CILE was fabricated as reference [38] and smoothed until its surface became mirror-like before modification. Then a mixture contained 1.0 $mg \cdot mL^{-1}$ GR-Pd nanocomposite and 30.0 $mg \cdot mL^{-1}$ Hb were prepared and vibrated for 5 min. 8 μL mixture were spread on CILE surface and dried naturally. Lastly 8.0 μL 0.5% Nafion solution was put on Hb-Pd-GR/CILE to get the final working electrode (named as Nafion/Hb-Pd-GR/CILE).

3. Results and discussions

3.1. Characterizations of materials

SEM images of Pd-GR nanocomposite on CILE were checked with its microstructure displayed in Fig. 1a. The nanosized Pd-GR composite with interconnected porous structure was exhibited and large quantity of Pd nanoparticles with uniform nanoscale were anchored on GR surface (Fig. 1b), which led to the augment of the active surface area. On TEM images of Pd-GR nanocomposite (Fig. 1c and d), plenty of Pd nanoparticles were distinctly and densely distributed on the typical GR sheets with partly overlapped and increased of particle size. XPS experiment was conducted in detail to study the chemical composition of Pd-GR nanocomposite with the results shown in Fig. 1e, in which the elements of C, O and Pd were well distinguished, indicating the immobilization of Pd nanoparticles on GR was realized. From the Pd spectra (Fig. 1f), two peaks at 335.0 eV and 340.4 eV could be denoted to $Pd3d_{3/2}$ and $Pd3d_{5/2}$ regions, which indicated the existence of Pd (0) in the Pd-GR nonocomposite. In addition, the appearance of two minor peaks at 337.6 eV and 342.8 eV showed another chemical state of Pd nanopaticles, which may be ascribed to the few formation of PdO_2 [39]. XRD patterns of Pd-GR nanocomposite were exhibited in Fig. 1g with well-defined characteristic peaks at $2\theta = 24.4°$ and 43.5°, which belonged to the (002) and (101) planes of GR. The peaks at $2\theta =$ 40.1°, 46.5°, 68.1°, 81.9° and 86.5° corresponded to the {111}, {200}, {220}, {311} and {222} planes of Pd (from JCPDS file No.46 to 1043) for a face-centered cubic structure, illuminating that the crystalline Pd nanoparticles were immobilized onto and/or into GR structure successfully without any noticeable impurity phases. From the intensity of the

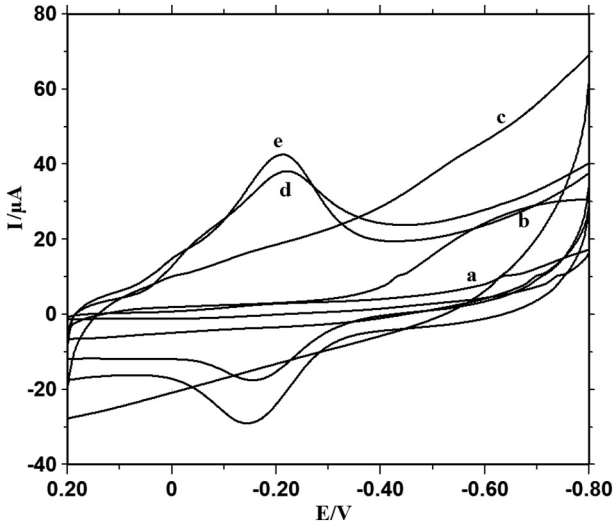

Fig. 3. Cyclic voltammograms of (a) CILE, (b) Nafion/CILE, (c) Nafion/Pd-GR/CILE, (d) Nafion/Hb/CILE and (e) Nafion/Hb-Pd-GR/CILE in pH 3.0 PBS at the scan rate of 100 $mV \cdot s^{-1}$.

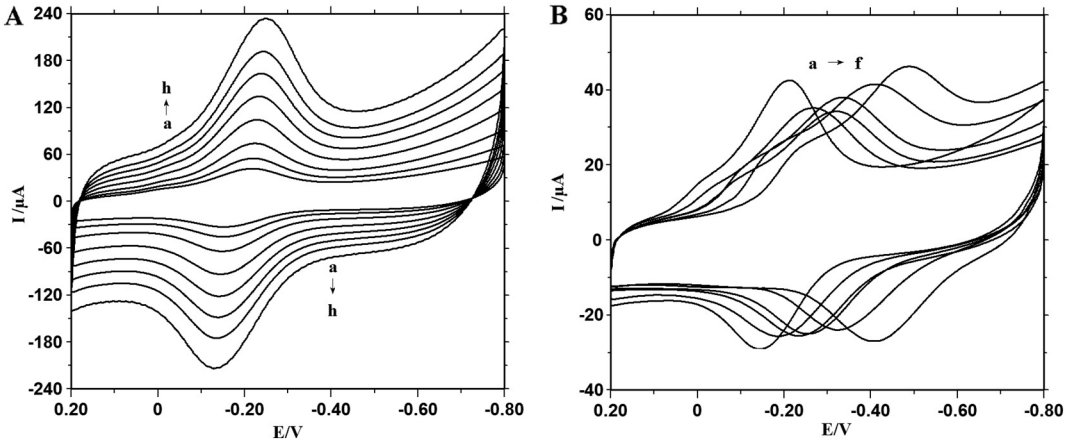

Fig. 4. (A) Influence of scan rate on redox responses of Nafion/Hb-Pd-GR/CILE in pH 3.0 PBS (scan rate from a to h as 100, 140, 200, 300, 400, 500, 600, 750 mV·s^{-1}); (B) Influence of pH on electrochemical responses of Nafion/Hb-Pd-GR/CILE at scan rate of 100 mV·s^{-1}(from a to f as 3.0, 4.0, 5.0, 6.0, 7.0, 8.0).

spectrum it can be known that the amount of Pd nanoparticles loaded in Pd-GR nanocomposite was high. The Raman spectrun of Pd-GR nanocomposite was shown in Fig. 1h with two characteristic bands at 1353.4 cm^{-1} and 1588.8 cm^{-1} appeared, which was well-marked as D and G bands. The intensity ratio of the D and G (I_D/I_G) was got as 0.97, which could be ascribed to the interaction of PdNPs with GR nanosheets [40].

3.2. Spectroscopic results

Spectroscopy is a simple way for identification of the secondary structure in hemoproteins [41]. The location of the Soret band can reflect the change of conformation in region of heme. As shown in Fig. 2A, UV–Vis absorption spectra of Hb (a) and Hb-Pd-GR mixture (b) gave the same characteristic Soret band at 405 nm. Therefore Hb kept its original structure and no denaturation or structural change occurred after mixed with Pd-GR nanocomposite. On FT-IR spectra the information of amide I (the stretching vibration of C═O in peptide chains of protein, 1700–1600 cm^{-1}) and amide II (the bending vibration of N—H and the stretching vibration of C—N, 1620–1500 cm^{-1}) can also reflect the change or denaturation of the secondary structure of the protein [42]. As shown in Fig. 2B, the positions of amide I and amide II in Hb (1647 cm^{-1} and 1543 cm^{-1}, curve a) were near to those of Hb-Pd-GR (1639 cm^{-1} and 1524 cm^{-1}, curve b), indicating no change of Hb structure. The slight movements of amide I and II could be recognized as the interaction of Hb with Pd-GR nanocomposite such as the hydrogen bonding or electrostatic interactions.

3.3. Direct electrochemistry

Direct electrochemistry of Hb on the modified electrodes was recorded in pH 3.0 PBS and the data were shown in Fig. 3. No redox currents appeared on CILE (curve a), Nafion/CILE (curve b) and Nafion/Pd-GR/CILE (curve c). On Nafion/Hb/CILE (curve d) a pair of well-defined redox peaks from heme prosthetic group Fe(III)/Fe(II) was observed with E_{pc} as −0.214 V and Epa as −0.143 V. The peak-to-peak separation (ΔE_p) was 71 mV, and the result reflected the realization of direct electron transfer of Hb with CILE. On Nafion/Hb-Pd-GR/CILE (curve e) the redox responses were enhanced with more symmetrical peak shape, showing the direct electron transfer was accelerated with the incorporation of Pd-GR nanocomposite. The presence of Pd-GR nanocomposite could form a better electron conducting pathway with large active surface area and synergistic effects. Therefore electron transfer from Hb heme Fe(III)/Fe(II) to the substrate electrode was enhanced with the responses became larger.

3.4. Electrochemical investigation

The influence of scan rate (v) on peak currents was checked with the results overlapped in Fig. 4A. A pair of symmetric peaks was observed at

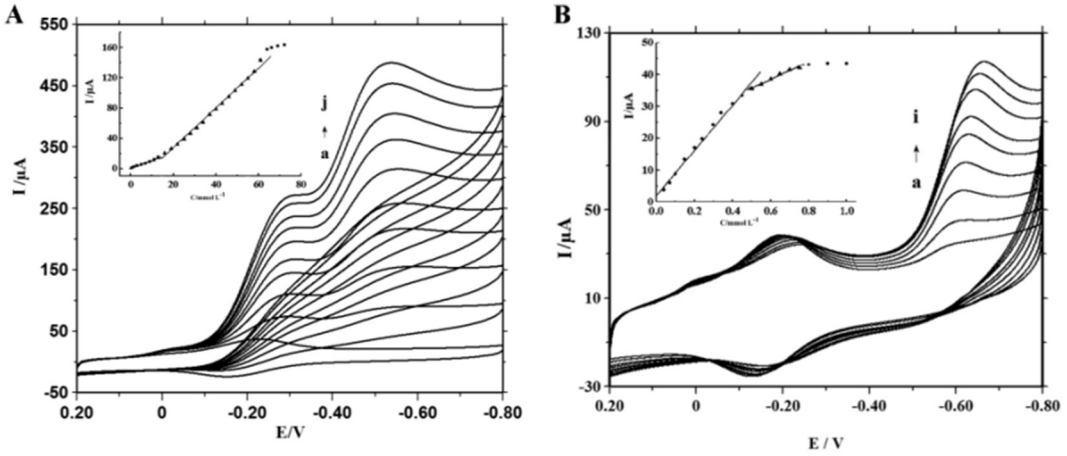

Fig. 5. (A) Cyclic voltammograms of Nafion/Hb-Pd-GR/CILE with TCA (from a to j as 3.0, 7.0, 14.0, 20.0, 28.0, 36.0, 44.0, 52.0, 60.0, 68.0 mmol·L^{-1}) in pH 3.0 PBS at the scan rate of 100 mV·s^{-1} (inset was the linear relationship between currents and the TCA concentration). (B) Cyclic voltammograms of Nafion/Hb-Pd-GR/CILE with $NaNO_2$ (from a to i as 0.04, 0.1, 0.2, 0.3, 0.4, 0.5, 0.7, 0.9, 1.1 mmol·L^{-1}) in pH 3.0 PBS at the scan rate of 100 mV·s^{-1} (inset was the linear relationship between currents and $NaNO_2$ concentration).

Table 1
Comparison of electrochemical parameters of different Hb modified electrodes to TCA detection.

Modified electrodes	k_s	Linear range ($mmol \cdot L^{-1}$)	Detection limit ($mmol \cdot L^{-1}$)	K_M^{app} ($mmol \cdot L^{-1}$)	Refs.
CTS/ELDH-GR-Hb/CILE	1.202	5.0–360.0	1.506	7.93	[34]
Nafion/GR-TiO_2-Hb/CILE	0.65	0.6–21.0	0.22	3.3	[50]
CTS-Hb-CNT-IL/CILE	0.84	1.6–12.0	0.4	6.572	[52]
CTS/TiO_2-Hb/CILE	1.62	0.8–32.0	0.26	1.75	[54]
CTS/CMS-Hb/CILE	0.95	2.0–70.0	0.30	1.60	[55]
Nafion/Hb-GO-IL/CILE	0.92	0.01–40.0	3.12×10^{-3}	0.0244	[56]
Nafion/nano-$CaCO_3$/Hb/CILE	0.75	0.6–12	/	2.57	[57]
Nafion/Hb-Pd-GR/CILE	0.96	0.6–61.0	0.35	0.63	This study

Note: MWCNT, multi-walled carbon nanotubes; CMS, carbon microspheres.

different scan rate ranging from 100.0 to 750 $mV \cdot s^{-1}$. The linear relationships were established with two regression equations as $I_{pc}(\mu A) = 108.06\nu\ (V \cdot s^{-1}) + 4.316$ ($n = 8$, $\gamma = 0.998$) and $I_{pa}(\mu A) = -148.37\nu\ (V \cdot s^{-1}) - 5.938$ ($n = 8$, $\gamma = 0.998$), demonstrating a surface-controlled process. From the equation $Q = nAF\Gamma^*$ [43], the surface electroactive Hb concentration (Γ^*) was obtained as 6.23×10^{-9} $mol \cdot cm^{-2}$, bigger than the theoretical monolayer surface concentration (1.89×10^{-11} $mol \cdot cm^{-2}$) [44]. The ΔE_p value increased along scan rate, indicating a quasi-reversible reaction process. The redox peak potentials had linear relationship with lnν, and the regression equations were $E_{pc}(V) = -0.0139 \ln\nu\ (V \cdot s^{-1}) - 0.237$ ($n = 8$, $\gamma = 0.991$) and $E_{pa}\ (V) = 0.0102 \ln\nu (V \cdot s^{-1}) - 0.136$ ($n = 8$, $\gamma = 0.993$). From Laviron's equations [45,46], the values of electron transfer coefficient (α) and the heterogeneous electron transfer rate constant (k_s) were evaluated as 0.42 and 0.96 s^{-1}.

The buffer pH has significant effect on cyclic voltammetric behavior of Hb and the curves were shown in Fig. 4B. Cyclic voltammograms changed gradually along with the buffer pH and the maximal current appeared in pH 3.0 buffer solution, which was selected as the supporting electrolyte. The change of buffer pH led to the movement of the peak potentials with good linear regression relationship of $E^{0'}$ and pH as $E^{0'}\ (mV) = -50.7\ pH - 10.2$ ($n = 7$, $\gamma = 0.995$). The slope (-50.7 $mV \cdot pH^{-1}$) was a little smaller than the theoretical value (-59 $mV \cdot pH^{-1}$) [47], demonstrating that proton was involved in the reaction.

3.5. Electrocatalytical activity

Electrocatalytical activity of Nafion/Hb-Pd-GR/CILE towards different substrates was investigated and shown in Fig. 5. As for TCA, the reduction peak increased gradually with the addition of TCA in the buffer solution (Fig. 5A), which was the typical electrocatalysis of redox protein [48]. A good linear relationship between the TCA concentration and the reduction peak current was got from 0.6 to 13.0 $mmol \cdot L^{-1}$ with the equation as $I_{ss}\ (\mu A) = 1.067C\ (mmol \cdot L^{-1}) + 0.193$ ($\gamma = 0.995$) and from 13.0 to 61.0 $mmol \cdot L^{-1}$ with the regression equation as $I_{ss}\ (\mu A) = 2.63C\ (mmol \cdot L^{-1}) - 24.78$ ($\gamma = 0.997$). The detection limit was got as 0.35 $mmol \cdot L^{-1}$ (3σ). The reduction peak current remained unchanged after the TCA concentration higher than 61.0 $mmol \cdot L^{-1}$, exhibiting a Michaelis-Menten dynamic mechanism. With the electrochemical form of Lineweaver-Burk equation [49], the apparent Michaelis-Menten constant (K_M^{app}) was calculated as 0.63 $mmol \cdot L^{-1}$. Table 1 compared the electrochemical parameters of Hb modified electrodes for the TCA detection.

Electrocatalytic reduction of $NaNO_2$ was also checked by cyclic voltammetry with voltammograms shown in Fig. 5B. The reduction peak observed at -0.59 V was resulted from electrocatalysis and the peak current increased gradually with $NaNO_2$ concentration. A linear relationship between $NaNO_2$ concentration and the peak current was got from 0.04 to 0.5 $mmol \cdot L^{-1}$ with the regression equation as $I_{ss}\ (\mu A) = 71.02C\ (mmol \cdot L^{-1}) + 2.038$ ($\gamma = 0.995$) and the detection limit as 0.2 $\mu mol \cdot L^{-1}$. Also the K_M^{app} for $NaNO_2$ reduction was calculated as 2.75 $\mu mol \cdot L^{-1}$. As shown in table 2, the electrochemical performances of Hb modified electrodes for $NaNO_2$ detection were summarized and compared.

3.6. Sample detection

The content of TCA in tap water sample at laboratory and medical facial peel solution were analyzed by the proposed method with the data shown in Table 3. Recovery of detection can be obtained by adding standard TCA solution into the samples. The relative standard deviation (RSD) were from 2.64% to 4.50% with the recovery from 96.17% to 101.24% for water sample and from 2.38% to 3.52% with the recovery from 99.52% to 107.23% for medical facial peel solution, respectively. Therefore the proposed electrode exhibited a potential and applicable way to utilize Nafion/Hb-Pd-GR/CILE for the detection of practical samples.

3.7. Repeatability and stability of Nafion/Hb-Pd-GR/CILE

The redox peak current stayed constant when Nafion/Hb-Pd-GR/CILE scanned for 50 cycles continuously in buffer solution. After stored at the 4 °C refrigerator for 4 weeks, cyclic voltammetric responses of the modified electrode remained 91.5% of the initial data, proving the excellent stability. Furthermore, seven detections of 5.0 $mmol \cdot L^{-1}$ TCA by one electrode gave the RSD value of 2.9% and six parallel fabricated electrodes used for the TCA detection with the RSD value of 3.6%. All the data indicated that Nafion/Hb-Pd-GR/CILE had a good repeatability.

Table 2
Comparison of electrochemical parameters of different Hb modified electrodes to $NaNO_2$ detection.

Modified electrodes	k_s	Linear range ($mmol \cdot L^{-1}$)	Detection limit ($mmol \cdot L^{-1}$)	K_M^{app} ($mmol \cdot L^{-1}$)	Refs.
Hb/RTIL/MWCNT/GCE	0.84	0.004–0.32	8.1×10^{-4}	/	[51]
CTS-Hb-CNT-IL/CILE	0.84	0.4–8.0	0.1	0.1	[52]
Hb-CS-DMF/GR/GCE	58.77	0.00055–0.033	1.8×10^{-4}	0.012	[53]
Nafion/nano-$CaCO_3$/Hb/CILE	0.75	/	/	0.22	[57]
Nafion/Hb-Pd-GR/CILE	0.96	0.04–0.5	0.0002	0.00275	This study

Note: RTIL, room temperature ionic liquids; CS-DMF, chitosan-*N*, *N*-dimethylformamide.

Table 3
Detection of TCA concentration in different samples ($n = 3$).

Sample	Detected ($mmol \cdot L^{-1}$)	Added ($mmol \cdot L^{-1}$)	Total ($mmol \cdot L^{-1}$)	Recovery (%)	RSD (%)
Tap water	0	2.00	2.02	101.24	4.50
		4.00	3.98	99.53	3.70
		6.00	5.77	96.17	2.64
Medical facial peel	43.19	1.00	44.26	107.23	3.40
		2.00	45.18	99.52	3.52
		3.00	46.21	100.67	2.38

4. Conclusion

Pd-GR nanocomposite and Hb solution was mixed and casted on CILE to get an electrochemical enzyme sensor. The high conductivity and good biocompatibility of Pd-GR nanocomposite provided an efficient electron channels for Hb to transfer electron with a pair of reversible and well-defined redox peak appeared on cyclic voltammogram. Electrochemical behavior of Hb was investigated with the parameters calculated. Due to the increased surface area and high conductivity, Pd-GR nanocomposite can adsorb more Hb molecules and meanwhile accelerate the rate of electron transfer. This novel Nafion/Hb-Pd-GR/CILE had great electrocatalytical activity towards different substrates including TCA or $NaNO_2$, and exhibited good properties including good stability, wide linearity range and low detection limit.

Acknowledgments

This project was financially supported by the National Natural Science Foundation of China (21365010, 21665007), the Program for Innovative Research Team in University (IRT-16R19), the National Natural Science Foundation of Hainan Province (2017CXTD007), the Fundamental Research Funds for the Central Universities (30916014103), and the Science and Research Key Project of Universities of Hainan Province (Hnky2016ZD-10).

References

[1] C. Léger, P. Bertrand, Chem. Rev. 108 (2008) 2379–2438.
[2] S.A. Bhakta, E. Evans, T.E. Benavidez, C.D. Garcia, Anal. Chim. Acta 872 (2015) 7–25.
[3] F.A. Armstrong, H.A.O. Hill, N.J. Walton, Acc. Chem. Res. 21 (2002) 407–413.
[4] S.E. Jorge, D.M. Ribeiro, M.N.N. Santos, M.D.F. Sonati, Hemoglobin: Structure, Synthesis and Oxygen Transport, Sickle Cell Anemia, Springer International Publishing, 2016.
[5] E.V. Suprun, V.V. Shumyantseva, A.I. Archakov, Electrochim. Acta 140 (2014) 72–82.
[6] A. Abo-Hamad, A.H. Alsaadi, M.M. Hayyan, I. Juneidi, M.A. Hashima, Electrochim. Acta 193 (2016) 321–343.
[7] Y. Zhang, J.B. Zheng, Electrochim. Acta 52 (2007) 7210–7216.
[8] W. Zheng, W. Chen, W.J. Weng, L.H. Liu, G.J. Li, J.W. Wang, W. Sun, J. Iran. Chem. Soc. 14 (2017) 1–8.
[9] F. Farjami, F.K. Mosalman, S. Ebrahimpourmoghaddam, H. Sharghi, Anal. Lett. 49 (2016) 1412–1423.
[10] S. Momeni, M. Farrokhnia, S. Karimi, I. Nabipour, J. Iran. Chem. Soc. 13 (2016) 1027–1035.
[11] E. Ye, X.J. Loh, Aust. J. Chem. 66 (2013) 997–1007.
[12] Z. Li, E. Ye, David, R. Lakshminarayanan, X.J. Loh, Small 12 (2016) 4782–4806.
[13] Q.Q. Dou, C.P. Teng, E. Ye, X.J. Loh, Int. J. Nanomedicine (**10**) (2015) 419–432.
[14] H.C. Guo, E. Ye, Z. Li, M.Y. Han, X.J. Loh, Mater. Sci. Eng. C 70 (2017) 1182–1191.
[15] R. Lakshminarayanan, X.J. Loh, S. Gayathri, S. Sindhu, Y. Banerjee, R.M. Kini, S. Valiyaveettil, Biomacromolecules 7 (2006) 3202–3209.
[16] R. Lakshminarayanan, E.O. Chi-Jin, X.J. Loh, R.M. Kini, S. Valiyaveettil, Biomacromolecules 6 (2005) 1429–1437.
[17] B.M. Teo, D.J. Young, X.J. Loh, Part. Part. Syst. Charact. 33 (10) (2016) 709–728.
[18] E. Ye, M.D. Regulacio, M.S. Bharathi, H. Pan, M. Lin, M. Bosman, K.Y. Win, H. Ramanarayan, S.Y. Zhang, X.J. Loh, Y.W. Zhang, M.Y. Han, Nano 8 (2016) 543–552.
[19] Q.Q. Dou, X. Fang, S. Jiang, P.L. Chee, T. Lee, X.J. Loh, RSC Adv. 5 (2015) 46817–46822.
[20] K. Huang, Q.Q. Dou, X.J. Loh, RSC Adv. 6 (2016) 60896–60906.
[21] C. Dhand, N. Dwivedi, X.J. Loh, A.N.J. Ying, N.K. Verma, R.W. Beuerman, R. Lakshminarayanan, S. Ramakrishna, RSC Adv. 5 (2015) 105003–105037.
[22] X.J. Loh, T.C. Lee, Q.Q. Dou, G.R. Deen, Biomater. Sci. 4 (2016) 70–86.
[23] H.C. Lee, W.W. Liu, S.P. Chai, A.R. Mohamed, C.W. Lai, C.S. Khe, C.H. Voon, U. Hashim, N.H.M. Said, Procedia Chem. 19 (2016) 916–921.
[24] X. Li, J. Yu, S. Wageh, A.A. Al-Ghamdi, J. Xie, Small 12 (2016) 6640–6696.
[25] Q.Q. Ke, J. Wang, J. Mater. 2 (2016) 37–54.
[26] N. Maleki, A. Safavi, E. Farjami, F. Tajabadi, Anal. Chim. Acta 611 (2008) 151–155.
[27] Q. Wang, Q.Y. Wang, K. Qi, T.Y. Xue, C. Liu, W.T. Zheng, X.Q. Cui, Anal. Methods 7 (2015) 8605–8610.
[28] C.L. Yang, X.H. Zhang, G. Lan, L.Y. Chen, M.W. Chen, Y.Q. Zeng, J.Q. Jiang, Chin. Chem. Lett. 25 (2014) 496–500.
[29] X. Ke, Y. Xu, C. Yu, J. Zhao, G. Cui, D. Higgins, Z. Chen, Q. Li, H. Xu, G. Wu, J. Mater. Chem. A 2 (2014) 16474–16479.
[30] Y. Huang, J. Lei, Y. Cheng, H. Ju, Biosens. Bioelectron. 77 (2016) 733–739.
[31] P. Shi, B.X. Wang, Q.L. Song, H. Wang, X. Liu, Z.Y. Bian, J. Electrochem. 21 (2015) 488–495.
[32] H.S. Dong, J.S. Lee, J. Jun, H.A. Ji, S.G. Kim, H.C. Kyung, J. Jyongsik, Sci. Rep. 5 (2015) 12294.
[33] M.A. Kumar, S.G. Patnaik, V. Lakshminarayanan, S.S. Ramamurthy, Anal. Lett. 50 (2016) 350–363.
[34] T.R. Zhan, X.J. Wang, X.J. Li, Y. Song, W.G. Hou, Sensor. Actuat. B-Chem. 228 (2016) 101–108.
[35] Y.P. Wen, W. Wen, X.H. Zhang, S.F. Wang, Biosens. Bioelectron. 79 (2016) 894–900.
[36] R. Mohammadrezei, H. Razmi, Sens. Lett. 14 (2016) 685–691.
[37] W.S. Zhao, X.Y. Li, Z.R. Wen, X.L. Niu, Q.F. Shen, Z.L. Sun, R.X. Dong, W. Sun, Int. J. Electrochem. Sci. 12 (2017) 4025–4034.
[38] X.L. Wang, L.H. Liu, W. Zheng, W. Chen, G.J. Li, W. Sun, Int. J. Electrochem. Sci. 11 (2016) 1821–1830.
[39] A.M. Venezia, L.F. Liotta, G. Deganello, Z. Schay, D. Horváth, L. Guczi, Appl. Catal. A 211 (2001) 167–174.
[40] M.R. Liu, C. Peng, W.K. Yang, J.J. Guo, Y.X. Zheng, P.Q. Chen, T.T. Huang, J. Xu, Electrochim. Acta 178 (2015) 838–846.
[41] K. Rosenheck, P. Doty, PNAS 47 (1961) 1775–1785.
[42] D.M. Byler, H. Susi, Biopolymers 25 (1986) 469–487.
[43] A.J. Bard, L.R. Faulkner, Electrochemical Methods, Fundamentals and Applications, second ed. Wiley, New York, 2001.
[44] S.F. Wang, T. Chen, Z.L. Zhang, X.C. Shen, Z.X. Lu, D.W. Pang, K.Y. Wong, Langmuir 21 (2005) 9260–9266.
[45] E. Laviron, J. Electroanal. Chem. 52 (1974) 355–393.
[46] E. Laviron, J. Electroanal. Chem. 101 (1974) 19–28.
[47] R.S. Nicholson, I. Shain, A. Chem, Anal. Chem. 37 (1965) 178–190.
[48] Y.H. Wang, C.M. Yu, H.Y. Gu, Y.F. Tu, J. Solid State Electrochem. 20 (2016) 1337–1344.
[49] W. Sun, D.D. Wang, R.F. Gao, K. Jiao, Electrochem. Commun. 9 (2007) 1159–1164.
[50] W. Sun, Y.Q. Guo, X.M. Ju, Y.Y. Zhang, X.Z. Wang, Z.F. Sun, Biosens. Bioelectron. 42 (2013) 207–213.
[51] W. Wei, H.H. Jin, G.C. Zhao, Microchim. Acta 164 (2009) 167–171.
[52] Z.H. Zhu, L.N. Qu, X. Li, Y. Zeng, W. Sun, X.T. Huang, Electrochim. Acta 55 (2010) 5959–5965.
[53] P. Liu, X.H. Zhang, L.J. Feng, H.Y. Xiong, S.F. Wang, Am. J. Biomed. Sci. 3 (2011) 69–76.
[54] F. Shi, W.C. Wang, S.X. Gong, B.X. Lei, G.J. L, X.M. Lin, Z.F. Sun, W. Sun, J. Chin. Chem. Soc. 62 (2015) 554–561.
[55] W.C. Wang, L.J. Yan, F. Shi, X.L. Niu, G.L. Huang, C.J. Zheng, W. Sun, Sensors 16 (2016) 6.
[56] W. Sun, S.X. Gong, F. Shi, L.L. Cao, L.Y. Ling, W.Z. Zheng, W.C. Wang, Mater. Sci. Eng. C 40 (2014) 235–241.
[57] W. Sun, R.F. Gao, K. Jiao, J. Phys. Chem. B 111 (2007) 4560–4567.